

Hydrodynamic study of a canting keel based appendage configuration.

C. López Pavón¹, R. Zamora Rodríguez², L. Pérez Rojas³

Abstract

Once the new rules that govern the design of VO70 class has been published, the necessity arises of evaluating the different configurations that this type of boats will adopt. These alternatives are mainly based in the incorporation of a canting keel to increase the righting moment of the boat, therefore to reach greater speeds. The handicap of having a greater righting moment is the lost of lateral force by the reduction of projected lateral area at the keel. To compensate this and to avoid excessive yaw angle, several solutions are being considered. In this article, the two most probable configurations to be adopted by the fore coming VO70 class will be evaluated.

Introduction

One of the main subjects during the process of yacht design is the ship stability. The heel position adopted to balance the moment from sails and appendages is a result of the force and moment equilibrium. Stability can be increased by a beamer hull (form stability) but this solution has the disadvantage of increasing drag associated with beamer hulls. Another way to achieve more stability, this one without changing hull's form, is to modifies the weight distribution (weight stability). The principal system used in offshore racing yacht to increase stability has been the ballast tanks; these are lateral tanks that can be filled with sea water to increase the righting arm. The principal disadvantage of this system is an increase in displacement. Other solution is lateral weights movement. The heaviest item in a racing yacht is the bulb, so a solution to increase stability is the lateral turn of the keel. This system is called canting keel.

The purpose of this paper is to present a study to evaluate a Canting Keel system (CK). The principal aim of this appendage configuration is to increase the righting moment by turning the keel and bulb to the windward side.

This system has been used for years in Open60 and Mini6.5 class designs. Recently the new Volvo Open 70 rule has allowed its use in Volvo Ocean Race. This fact is a good platform for research and development of this system. In ETSIN's towing tank an investigation has begun to improve the knowledge on this field.

First of all, the VPP (Velocity Prediction Program) developed in the ETSIN had to be adapted to evaluate the new variant introduced with the rotation of the keel.

Yachts equipped with canting keels have some problems associated with the loss of lateral force with the keel canted. To increase this loss, these designs use to incorporate some appendages to generate more lateral force. Two of these variant are evaluated in this investigation. To have a previous performance of this configuration, the appendage was studied using a 2D CFD.

In order to put some light in this topic, towing tank tests were made with a bare hull adapted to allow these appendages configurations. The results of the towing tank test can be used to feed the VPP and refine the performance prediction of the yacht.

VPP Modifications

When a sailing yacht has to be evaluated, is essential a VPP tool's help to make balance between hydrodynamic and aerodynamic forces. The VPP developed in ETSIN calculates forces and moments on sails using experimental data (IMS sail coefficients). The hydrodynamic conditions

Canal de Ensayos Hidrodinámicos. E.T.S.I. Navales.

¹ clopez@etsin.upm.es

² rzamora@etsin.upm.es

³ lperezr@etsin.es

are calculated to balance sails forces and moments using mathematical models similar to the IMS ones. This calculation is carried out by a Newton-Rapson iterative method.

The most important effect over the yacht of a CK system is the righting arm increase. Turning the keel and bulb mass to the windward side generates an extra righting arm. This makes the yacht adopt more vertical positioning, allowing the sails increase their efficiency, hence obtaining more speed. Keel's rotation induces as well the elevation of the vertical centre of gravity (VCG), which is a potentially dangerous situation if the yacht gets into a high wind speed zone (the reserve of stability is reduced, see figure 1) Also a non desirable reduction in the vanish stability angle occurs.

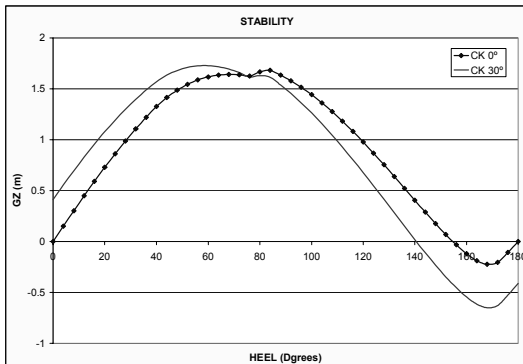


Figure 1

To evaluate stability conditions of a yacht equipped with this canting keel system, naval architecture software can be used. The bulb and keel mass can be lifted up and moved from the centre line to a side (figure 2) in this modification the ship has a slightly different stability curve. The VPP can analyse yacht's performance for that single condition. The calculation made with that stability curve does not simulate a real sailing condition, in lights wind and downwind sailing the heeling moment is minimized, so the use of canting keel is not necessary. For every sailing condition there is an optimum canting keel angle, the assumption of a fixed canting keel angle for all conditions is erroneous. The best solution to be used in a VPP is the correction of the previously calculated stability curve at 0° CK rotation to choose the best CK angle in every sailing condition. The correction is made in the GZ curve.

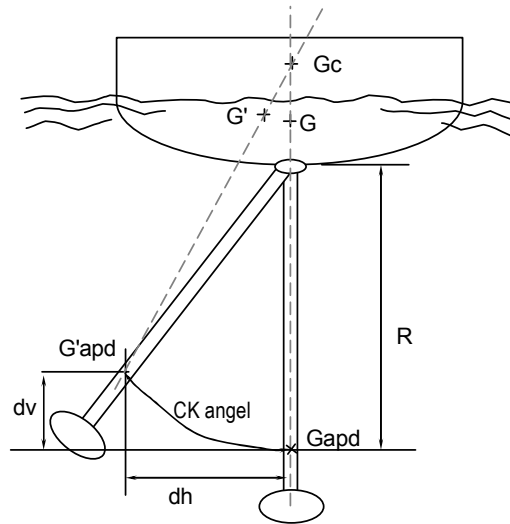


Figure 2

G: centre of gravity of yacht.
Gc centre of gravity of yacht without keel and bulb.
G'apd: Centre of gravity of keel and bulb.
R= distance from keel centre of rotation to G'apd.

In the upright condition we can calculate the variation on G'apd:

$$dv = R(1 - \cos(\text{CK_angle}))$$

$$dh = R \cdot \sin(\text{CK_angle})$$

When the VPP evaluates a heeled condition, the program calculates the increase in the GZ curve previously obtained with the keel fixed at 0° CK.

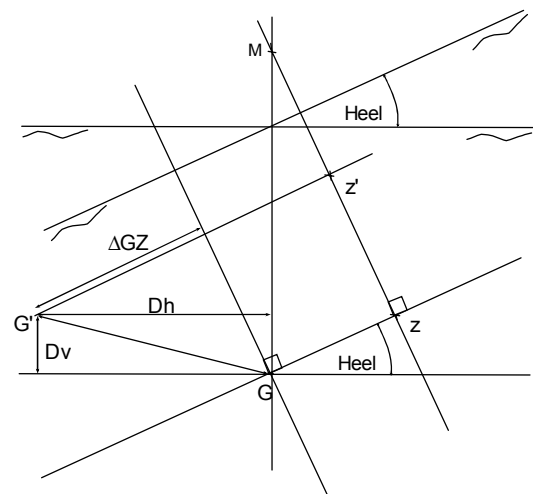


Figure 3

$$D_v = d_v \frac{(\text{keel \& bulb})\text{weight}}{DSPL}$$

$$D_h = d_h \frac{(\text{keel \& bulb})\text{weight}}{DSPL}$$

$$\Delta GZ = D_h \cos(\text{Heel}) - D_v \sin(\text{Heel})$$

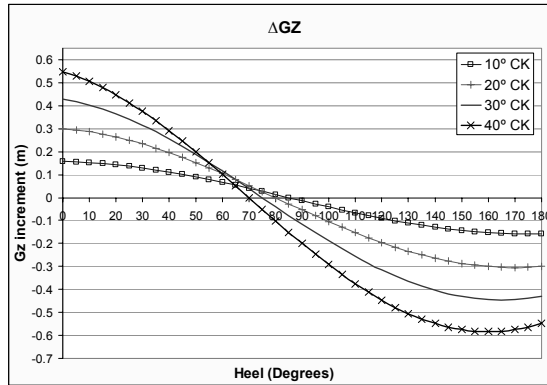


Figure 4

The VPP starts the analysis with the CK at 0° as a fixed keel. Once the equilibrium position is found for a determined condition of true wind angle (TWA) and true wind speed (TWS), the program saves the calculated speed and changes the CK angle a small amount. This new condition with the same TWA and TWS gives a different equilibrium condition. We compare the previous solution with last one and if more speed is obtained, we continue with another loop, changing the keel angle again. This loop is made until we obtain lees speed or until we obtain the maximum canting keel angle.

This procedure is shown in the next diagram.

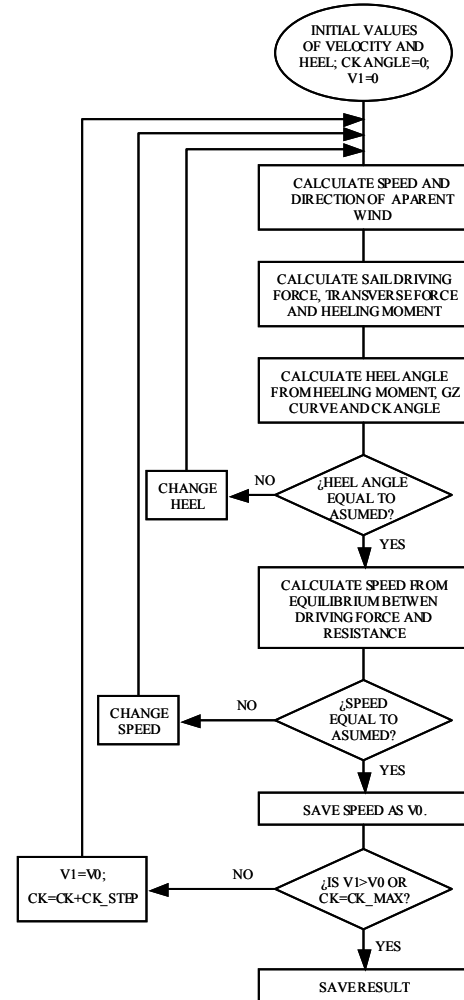


Figure 5

The sails have to be tuned to achieve real performances. If the maximum sail area is maintained over all true wind angles, the yacht could find some extreme heeled conditions. In these conditions, it is known that a reduction in sail flat or reef provides improvements in speed and heel conditions. In order to optimise this sail trimming in VPP, there are loops in sail reef and sail flat.

A certain leeway can be obtained as a consequence of sail's lateral force. This force has to be balanced with the lateral force generated by the lift in appendages. This lift, in conventional appendage configuration, is obtained due to the attack angle generated by leeway in keel, and a rudder angle of attack.

The use of this VPP allowed estimations for the sailing conditions of the yacht. First we obtained the fundamental parameters of the canoe body using naval architecture software. These data are used to calculate a

residual resistance curve of the canoe body using Delft IV Systematic Yacht Hull Series. Also the geometry of the appendage is needed to complete drag's calculation over the hull.

To obtain a stability curve, the vertical centre of gravity position (VCG) is needed. This parameter can be obtained with a weight distribution or estimated by previous experience in similar types of yachts. The stability curve is obtained with the keel fixed at 0°. Also the program is provided with the sail geometry and appendage characteristics, and it is ready to start the yacht's velocity prediction calculation.

VPP Evaluation

To evaluate the advantage of a canting keel system, first we need to obtain the yacht's performance without it. Fixing the maximum CK angle at 0° we evaluate this condition. With sail geometry, just as used in VO70, a Boat Speed (BSP) polar curve is obtained. In the same conditions, we can calculate another polar including the canting keel system effects (Fig 6).

Both polar curves can be compared, and a reduction in the heel angle for the CK system is observed (Fig 7).

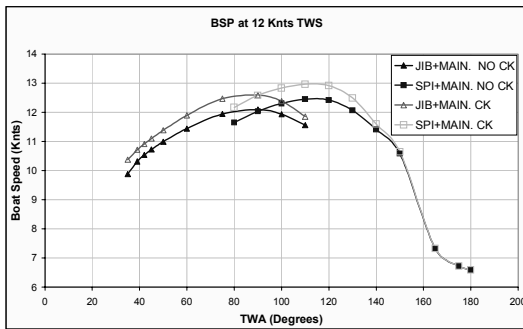


Figure 6

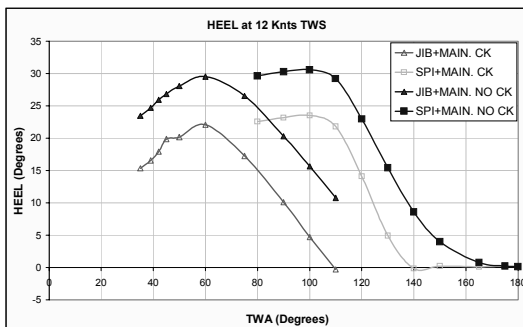


Figure 7

Speed boat has been compared and a difference in half a knot sailing at 12 knots of TWS has been found. This polar curve is obtained with the VPP assuming that lateral force can be balanced with the one generated by the appendage.

This is true supposing that the yacht adopts a leeway angle in order to achieve this lateral force. One of the problems using a CK system is losing projected lateral area that hence can't be used to generate lateral force. In a conventional yacht, this lateral force is generated mainly by in the keel and the rudder.

The reduction of lateral projected area makes the yacht adopts a bigger leeway angle equilibrium condition. It can be observed in figure 8 how the lift (L2) has to be higher than (L1) to obtain the same lateral force (L_f) with the keel rotated.

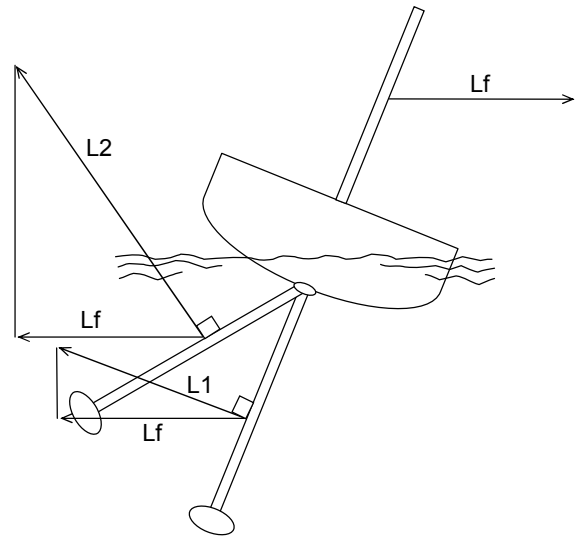


Figure 8

Increasing leeway angle and lift has two main undesirable effects; i.e., a drag increase on the canoe body (associated with non-linear lift) and the increase on induced and viscous drag over the appendage.

The solutions adopted to reduce leeway angle come from setting up another lifting surface to generate an extra amount of lateral force. In modern design, two solutions are chosen. The first one is the addition of a forward foil (fig 9) in the yacht's centreline. This appendage can rotate as a rudder and in this paper will be named forward rudder.

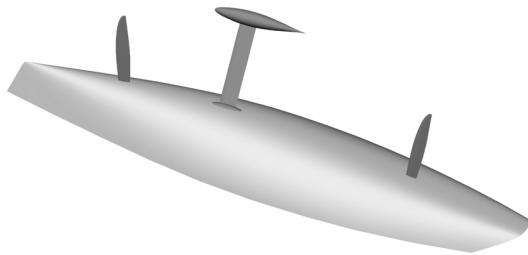


Figure 9

The second solution, used in Open60 and Mini650 yachts, is a non symmetrical retractable foil (Dragger Board, DB) (Fig10) These yachts have two of these foils, on in each side. When the yacht heels, the leeward foil are used to generate extra lateral force and the windward foil is lifted up to reduce drag.

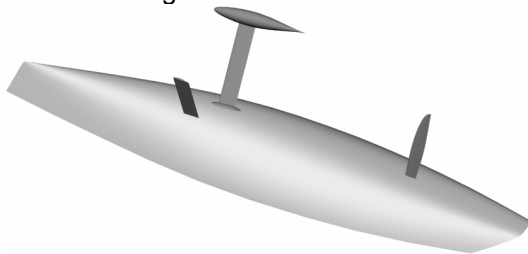


Figure 10

Appendage performance

In order to analyse appendage shapes, a 2D section analysis is widely used, this method gives the drag and lift coefficients for 2D foils. These coefficients can be corrected to obtain 3D performances with a good agreement with experiments. One of the most used codes to analyse 2D sections is XFOIL. This code uses a high order panel method to calculate the inviscid flow over foils, coupled with an integral boundary layer method.

This code has been used to obtain the characteristics of the keel and rudder. The geometry sections (NACA 0014 and NACA 0012) were computed and the C_l and C_d coefficient were obtained for a wide range of attack angle. The forward rudder was selected from the stock of our basin (NACA 0012), Its characteristics are similar to the aft rudder, with a 15% higher lateral area.

The dragger board to be evaluated was designed as a non symmetric foil. This kind of foils can generate more lift with less drag than a symmetrical rotatory foil. To select the section shape, eleven candidates were tested with XFOIL. These geometries were

selected from NACA and Eppler database with a thickness of 10% of their chords. The best performances were found for Eppler392 whose C_d/C_l-C_l curves presented the most efficient characteristic. These curves were calculated at Reynolds $3e6$ in the selection process (Fig 11) and $Re 1e5$ to use in the extrapolation process. The graphics for different Reynolds showed a similar behaviour in the lift versus attack angle (Alfa) curves (Fig 12) , but the viscous drag versus “alfa” curves are different (Fig 13), therefore an extrapolation process is needed to interpret the data obtained from the towing tank. If results tests are used directly to evaluate a design, the viscous drag is going to induce an overestimating of total drag.

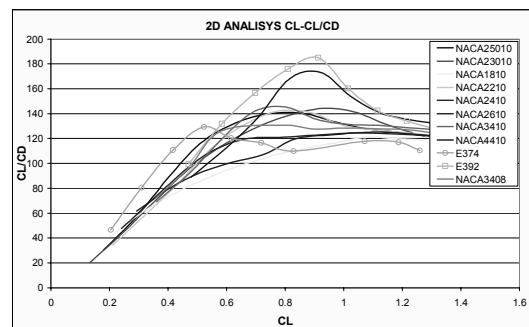


Figure 11 (Colour Fig)

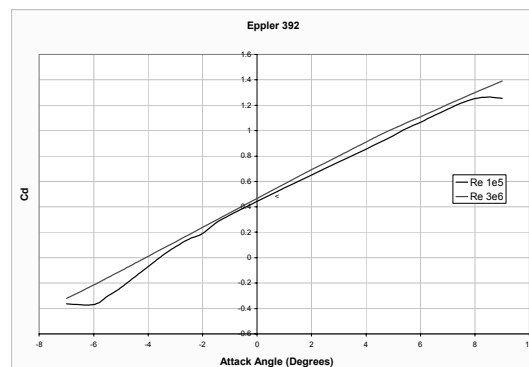


Figure 12

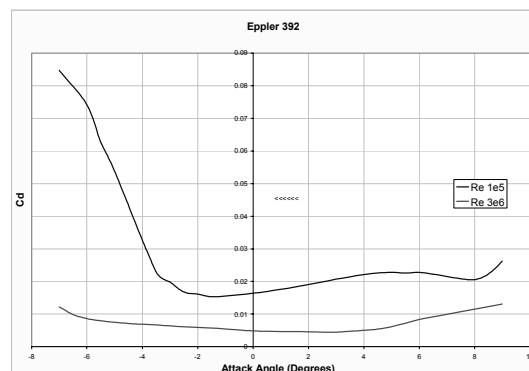


Figure 13

The main dimensions of the dragger board were selected in order to have the same lateral area that the rotatory forward rudder and with enough thickness to be built. Final dimensions of the dragger at full scale are:

Section: Eppler 392.
Thickness: 70mm
Chord: 700mm
Span: 1960 mm

Aimed at having a first evaluation for both appendages' configurations, an estimation of induced and viscous resistance was made over the appendages at full scale. The process began choosing the test speed, heel, and lateral force to be balanced. This force can be reached with different conditions in attack angle, appendages and leeway angle. First, we chose forces distribution between back rudder and the rest of appendages. With this load a 3D Cl coefficient can be deduced for the back rudder.

$$Cl_{3D} = \frac{L}{0.5 \cdot \rho \cdot A_L \cdot V^2}$$

A_L = Lateral Area of appendage.

To obtain the 2D Cl, the effective aspect ratio is needed, for a first analysis this coefficient can be calculate as twice AR ($AR = \text{Span} \cdot \text{Chord}$).

$$Cl_{2D} = Cl_{3D} \left(1 + \frac{2}{AR_E}\right)$$

AR_E = Effective aspect ratio = $2 \cdot AR$
 L = Lift.

With this coefficient and the previously calculated Cl- α curve, the attack's angle for the rudder is predicted.

The treatment for the rest of the lateral force is similar. The heel and the canting keel angle under evaluation, define a lateral projected area for the canting keel and the forward appendage (dragger board or front rudder). For a given angle of this appendage, selected previously, an iteration process on the leeway angle is started, and an equilibrium solution is found. In this solution the lateral force is the one that had been previously assumed. This solution's leeway angle gives a load distribution between keel and forward appendage (DB

or Front Rudder). All this calculation process is repeated changing the angle for the forward appendage respect to the flow.

With this analysis we have a data matrix whose entries are: back rudder angle of attack with respect to the stream, forward appendage angle of attack and the corresponding leeway angle calculated for this condition. Once the leeway is calculated for every point, the induced and viscous resistance are calculated for the three appendages. The induced resistance is derived by a semi-empirical model.

$$Ri = \frac{0.5 \cdot \rho \cdot V^2 \cdot A_L \cdot Cl_{3D}^2 \cdot (1 + \sigma)}{\pi \cdot AR_E}$$

$(1 + \sigma)$ = Correction factor for non-elliptical distribution on lifting surface [2]

$$Rv = 0.5 \cdot \rho \cdot V^2 \cdot A_L \cdot Cd$$

The sum of Rv and Ri is normalized with the square of the velocity times the density (dynamic pressure). This variable is plotted in terms of the back rudder attack's angle with respect to the flow and forward appendage attack's angle.

To summarize, the sequence is as follows:

- A total lateral force to be generated by the appendages is selected (VPP, Experience...).

- The lateral force is distributed between back rudder and the rest of appendage, normally from 0% to 40% in 2% steps of the lateral force generated in the rudder. 20 points to evaluate are generated.

- For every previous point, the rudder attack's angle to the flow is calculated, using the 2D Cl corresponding to the rudder previously calculated with XFOIL and taking into account 3D corrections for Cl. Also, the Viscous and Induced drag are calculated for the back rudder

- The rest of the lateral force has to be generated by the keel and the forward appendage (Dragger board, or front rudder).

- Since the dragger board is a non rotatory foil, It is set up an attack angle respect to the hull. The lateral force has to be generated by this appendage and keel thanks to the

leeway. In an iteration process, required leeway is calculated. (The attack angle of the DB will be; leeway plus the attack angle to the hull) Again, the Viscous and Induced drag is calculated for these appendages.

.- This operation is repeated for all the twenty points of %loads in the rudder, changing the DB angle of attack, and therefore, a matrix is obtained.

Appendage resistance: CK 0° + Dragger Board 11Knts Boat Speed

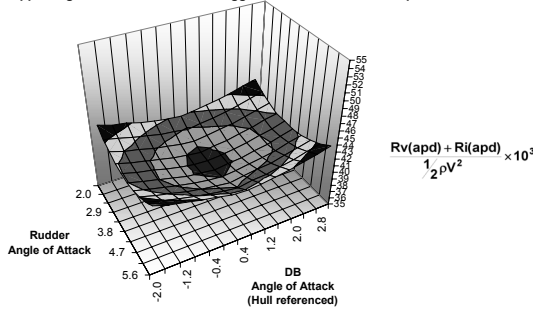


Figure 14 (Colour Fig)

Appendage resistance: CK 30° + Dragger Board 11Knts Boat Speed

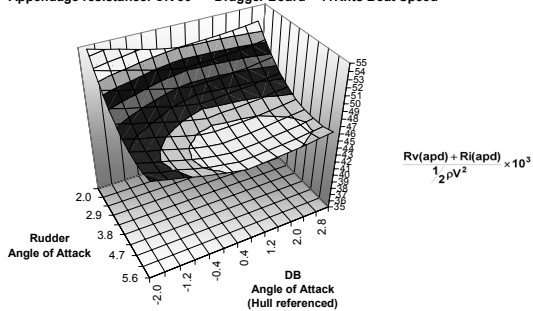


Figure 15 (Colour Fig)

.- In the case equipped with the forward rudder, rotating the foil allows to have independence between the leeway angle and forward rudder position. For an angle of attack of this foil, the lateral force is evaluated and the remaining force has to be generated by the keel through a leeway angle. The final matrix stores for a range of turn angle in rudder and turn angle in forward rudder, the induced and viscous drag over the appendages' system.

Appendage resistance: CK 0° + Forward Rudder 11ktns

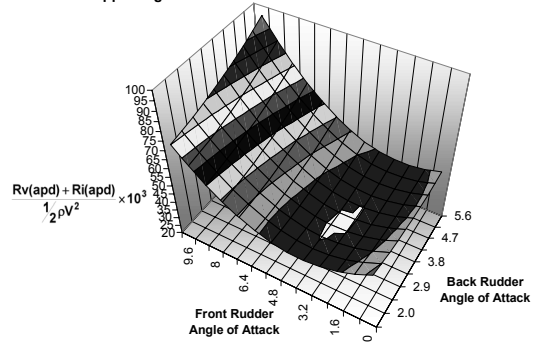


Figure 16 (Colour Fig)

Appendage resistance: CK 30° + Forward Rudder 11 ktns

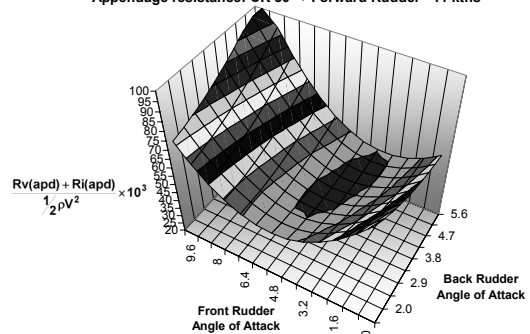


Figure 17 (Colour Fig)

This matrix provides help to program the use of the front rudder. The difficulties of this system are infinite equilibrium conditions that can be found with two rotatory appendages. The position of both appendages aim at reducing yacht's resistance. A first approximation to select the minimum drag position can be the process described before. If the viscous and induced drag is plotted, (Fig 16) a hollow shows the optimum angle with respect to the flow for the dragger and the back rudder. It is Important to notice the increase in resistance obtained with the CK at 30° (Fig 17). This is because of the increase on the induced drag. The keel generates less lateral force maintaining similar lift and this reduction in lateral force has to be compensated with greater leeway. This implies that the lift in the keel has to be increased (supposing that the attack angle in the rest of appendage could be maintained), an hence the induced drag grows up in keel.

In figure 17, with a 30° canted heel, this effect is clearly shown. For the same lateral

force, the optimum configuration has a greater resistance.

For the DB equipped case (figures 14, 15), the problem is similar, but once the attack angle of the foil is selected, in sailing conditions there is only an equilibrium configuration once the rudder is fixed. The boat yaws to find this equilibrium position. The balance between a given sail force and the hydrodynamic force is controlled by the rudder.

		DAGGER BOARD Eppler 392		FORWARD RUDDER	
		CK 0°	CK 30°	CK 0°	CK 30°
RUDDER	(Degrees respect to the inflow stream)	3.8	4.2	2.9	3.8
LEEWAY	Degrees	2.8	3.6	2.6	2.1
D-B angel	(Degrees respect to the hull)	0.8	0.8		
FORWARD RUDDER	(Degrees respect to the inflow stream)			3.2	4
RESISTANCE	$R_{vapp} + R_{lapp}$ $0.5\rho V^2 \cdot 10^3$	39.82	44.17	39.7	43.5
RUDDER	Laterla force distribution; %Total laterla Force	29%	33%	21%	30%
CANTING KEEL		40%	31%	42%	24%
FORWARD FOIL		31%	36%	37%	46%

In the table above there is a summary of the main conditions for using the appendages. For the DB, there is only one attack angle respect to the hull (it is a retractable appendage, non rotatory) and therefore, we have selected an average position (0.8°) between the minimum drag with the CK at 0° (Fig 14), and with the CK at 30° (Fig 15).

It is important to study the load distribution between appendages. The more distributed the load, the minimum the induced drag. So the table above show a clear increment in drag when the keel turns one side. This turn needs to be compensated by a greater load in the keel and the rest of appendages so that the induced drag increases.

Model test

Towing Tank tests were made with a 1999 Americas Cup model. This 1:7 scale model was modified to host a canting keel. A new keel and bulb were made for this purpose. Also supports for a forward rudder and a lateral appendage were fitted to make the test with these configurations possible.

The main characteristic of the full size yacht are:

DSPL	20180	(kg)
LWL	18.21	(m)
BWL	3.53	(m)
T	0.81	(m)
WSA	50.69	(m ²)
Cp	0.529	
LCB	54.5	% LWL

Test facility

Tank tests were made in model basin of the Naval Architecture Department of the Universidad Politécnica de Madrid. This has the following dimensions: 100 m long by 3.8 m wide by 2.2 m deep. It was constructed in 1967 and was updated by increasing its size some years later. It has a digital controlled carriage with a range of velocities up to 3.5 m/s. Sailboat model testing began in 1981 with a yacht test for the Withbread, and continued through 1992 with tests for Spanish America's Cup syndicate. This research was extended in 1995 and 1999 America's cup editions. These participations allowed the towing tank to gain experience and new yacht testing equipment.

Model preparation

For this test, a 1999 scale model was used. This model is one of the beamest on the 1:7 America's Cup series that were tested for the Spanish syndicate for that edition of the event. It also has a destroyer bow and this mean that it is similar in shape and length to the VO70 yachts. The modifications made to the model were the removing of the attachments in the fixed keel and the construction of supports for the Canting keel axis. A internal box was also laminated in order to control the amount of water that comes in trough the seal between the hull and the CK support. The keel has a plan form with a NACA 0012 section a chord of 100 mm and a span of 430 mm at model scale. The bulb is a NACA 65015 revolution surface, 500 mm long. The hull has turbulent stimulators (studs) 3.15 mm diameter, 2.55 mm high separated 15 mm and located in the first of the 20 sections the hull is divided on. Keel and bulb have the same studs separated 10 mm and located at 25% of the chord length from the leading edge.

The CK adopts a maximum angle of 30° each side. For it's tuning a screw bar is

used. This piece is fixed to one side of the model and at the end of the keel by a pair of nuts.

Experimental procedure

The model was tested using the procedure originally developed by Davidson at the Stevens Institute of Technology. This procedure allows heave and pitch movement of the yacht during the test. To measure drag, lift, roll moment and yaw moment, a 4 component dynamometer was used (Fig 30). This device is based in 6 load cells. Two of these cells measure forces in the transversal direction (y) aimed at calculating lateral forces and the hydrodynamic centre of pressure position. Another load cell aligned with the towing tank, measures drag. The three remaining cells are used to calculate the dynamic heeling moment during the test running.

This dynamometer is set up on the model deck, and it is linked to the carriage by an articulated arm that allows heave and pitch movements. Trim is measured by two lasers that indicate the movements at bow and stern.

Calibration

Dynamometer is calibrated before its installation on the model. For this purpose, a table exists where the dynamometer is hanged on. Calibration procedure consists of pulling from every cell with a calibrated weight. In individual cells the moment derived is theoretically zero by the use of flexible links. In practice, the measured crosstalk does not approach that limit and a correction has to be set up in the acquisition data software. This crosstalk can be measured as the amount of load measured in one cell when another cell is excited with a force in its measurement direction. To calculate the complete crosstalk, a 6x6 coefficients matrix has to be measured. This matrix is used during data acquisition to adjust the measurement made with the dynamometer.

Once the dynamometer is calibrated, it is fixed on the model and the articulated arm is attached to the carriage. To align the model with the carriage direction, a laser aligned along the carriage direction is used. This 0°

leeway point is corrected with a few carriage runs with at $\pm 1^\circ$ leeway. This runs allow determining the zero lift angle. When the model is well aligned the rudder may be added to the model and similar runs, changing angle of attack, determine the neutral angle of the rudder or any other appendage to be tested.

Test results

The results shown here are for a 20° heel condition. This is a significant sailing condition, as demonstrated by the VPP (figure 6).

The resistance graphs represent the percentage increment compared with the first condition tested in every plot, taken as a reference. The runs codification is as follow:

CK: Canting Keel angle (degrees)
H: Heel angle (degrees)
L: Leeway angle (degrees)
R: Rudder angle (degrees)
FR: Front Rudder angle (degrees)
DB: Draggeer Board angle (degrees)

The extrapolation method uses ITTC line to calculate frictional resistance in the canoe body. A form factor of 1.1 was used to calculate viscous resistance over the canoe body. The appendage viscous resistance was calculated using the 3D Cd previously calculated for every appendage and for every condition (towing tank and full size). Induced resistance over each appendage is calculated using Ci derived from the same analysis as Cd. Interference resistance associated with hull-appendages interaction is not taken into account for this extrapolation. Effects of appendages downwash on other appendages are calculated using formulation proposed in [2]. The residual resistance calculated in this paper includes the wave making resistance and the viscous pressure resistance.

The full scale results for the yacht equipped with rudder and canting keel only (figures 23, 24) show the least resistance for the 0° leeway 0° CK conditions. When the keel turns 30° in the same conditions, the drag increases. In the 3° leeway conditions, the results change and the 30°CK show better performance (figure 23). These results have its explanation in the characteristic wave pattern. The CK turn and the leeway

adopted, changes the wave pattern and the wave drag. Another drag source is the one associated to appendages downwash interference. The effect of the wake generated in the keel over the rudder flow is evaluated by empirical models that reduce the attack angle and the rudder inflow speed [2]. These models were developed for fixed keels. In the extrapolation method used in this paper, this reduction has been calculated for 0° CK condition (as a fixed keel). In the 30° CK case, no interference between keel and rudder has been supposed. For the front rudder case a similar treatment was followed to calculate attack angles and velocities induced by appendages interferences.

The residuary resistance (figure 24) is the total resistance minus induced and viscous drag. It represents the resistance associated with the wave pattern formation as well as other resistance associated with hull forms (viscous pressure resistance). The residuary resistance plot shows an increase in it for the 3° leeway conditions. For these conditions, the residuary resistance is reduced when the keel is turned. This behaviour is justified by the variation on wave pattern when the keel is turned. This conclusion is different for the 0° leeway condition. In this case, the form drag is increased when the keel is turned.

The front rudder case is analysed for two different conditions. One with no leeway and both rudders rotated 6° and another with 3° leeway (figure 21, 22). The first condition was tested to evaluate the performance of the yacht in a zero leeway condition, where the lateral forces are generated by both rudders. For this situation, the induced resistance is bigger than the 3° leeway one, in which the lateral force is distributed among the three appendages. The zero leeway and 6° rudders rotation, may be thought as the best solution in drag reduction. The total drag plot demonstrates that this fact is not correct. The 3° leeway runs show less drag than the 0° leeway because the difference in wave drag caused by the forward and back rudder at 6° is greater than the extra wave drag generated by a 3° leeway for the low speed runs. The CK shows similar behaviour as the one described by the test without dragger nor forward rudder. The 30° canting keel test shows less drag for 3° leeway and a slight increase for the 0° leeway conditions.

The yacht with dragger board was analyzed with two different leeway angles 1.5° and 3°. The relative attack angle of the dragger is 0.8° as was theoretically calculated (figure 19, 20). Examining the total resistance curve (figure 27) a similar behaviour like the one above was found. The CK rotation has drag benefits for the higher leeway conditions and drag increase for the less leeway one. The higher leeway produces a global increase compared to the 1.5° leeway conditions.

The maximum total drag increase produced by 30° canting keel rotation compared to the 0° rotations is fewer than 3% in all cases. In the higher leeway conditions this rotation has shown to lead to a reduction in drag.

VPP

The maximum increase of drag calculated for a rotated canting keel has been 3% over the total drag. For a first estimation of how this increment affects the performance calculated in the VPP, a global increase of 3% in total resistance was set up in the program in order to have an evaluation of the speed lost when the CK turns. A reduction in performances was obtained, but the CK system still allows more speed than the fixed keel (figure 29).

Conclusions

A procedure to analyse different appendage configurations has been devised and tried by the ETSIN model basin staff. This procedure has included the upgrading of VPP and the use of CFD to calculate 2D performances of appendages sections. These characteristics are used to calculate 3D induced and viscous drags at the model and full scale, so this way traditional extrapolation process can achieve more precision in this field. The area that requires more research is the interference between appendages downwash. It seems to be crucial to analyze configurations as a canting keel.

First tests show a better drag comportment for the keel rotated when the leeway increases. For low leeway angle, the increase in drag when the keel rotates reduce global

performance of yacht, but maintaining advantage over a yacht without CK.

This investigation have just started and the next item will be the extrapolation method upgrading. The flow interactions between appendage and wake generated by forward appendages needs to be studied. This area will be improved by the use of RANS cfd codes.

Future detailed investigation in these topics will be over a VO70 model designed and tested in ETSIN Towing Tank.

References

[1] Parsons, B.L., Pallard, P., "The Institute for Marine Dynamics Model Yacht Dynamometer". 13th Chesapeake Sailing Yacht Symposium, SNAME, pp. 153-164, 1997.

[2] Van Oossanen, P., "Predicting the speed of sailing yachts". Trans. SNAME, pp. 339-397, 1993.

[3] Milgram, JH., "Fluid mechanics for sailing vessel design". Annu. Rev. Fluid Mech, pp. 613-653, 1998.

[4] Gerritsma, J., Keuning, J.A. and Versluis, A., "Sailing Yacht Performance in Calm Water and Waves" 11th Chesapeake Sailing Yacht Symposium, SNAME, pp233-245, 1993.

[5] Teeters, J.R., "Refinements in the technique of Tank Testing", 11th Chesapeake Sailing Yacht Symposium, SNAME, pp13-34, 1993.

[6] Frank DeBord, Jr., Jim Teeters., "Accuracy, Test Planning and Quality Control in Sailing Yacht Performance Model Testing", New England Sailing Yacht Symposium, 1990.

[7] Offshore Racing council. "Formulations of the IMS, International Measurement Rule" April 2003.